Factor XIIa as a novel target for thrombosis: target engagement requirement and efficacy in a rabbit model of microembolic signals

Christopher M. Barbieri, Xinkang Wang, Weizhen Wu, Xueping Zhou, Aimie M. Ogawa, Kim O'Neill, Donald Chu, Gino Castriota, Dietmar A. Seiffert, David E. Gutstein, Zhu Chen

In Vitro Pharmacology (C.M.B., A.M.O., K.O., D.C.), Cardiometabolic Diseases (X.W., W.W., X.Z., G.C., D.A.S., D.E.G., Z.C.), Merck &Co., Inc., Kenilworth, NJ USA

Running Title Page:

a) Running Title: FXIIa inhibition by rHA-Mut-inf

b) Address Correspondence to:

Zhu Chen, Ph.D., Cardiometabolic Diseases, MRL, K15-C409, Galloping Hill Road, Kenilworth, NJ 07033, USA Tel: (908) 740-0642 Fax: 908-740-4020; Email: zchen17@hotmail.com

c) The number of text pages: 30

The number of tables: 2

The number of figures: 6

The number of references: 46

The number of words in Abstract: 249

The number of words in Introduction: 697

The number of words in Discussion: 1344

c) A list of nonstandard abbreviations:

aPTT: activated partial thromboplastin time; FXa: Factor Xa; FXIIa: Factor XIIa; MCA: middle cerebral artery; MES: microembolic signals; PT: prothrombin time; rHA-Mut-inf: recombinant human albumin-tagged Mutant infestin4; TCD: transcranial Doppler; TIA: transient ischemic attack

A recommended section assignment: Cardiovascular

Abstract

Coagulation Factor XII (FXII) plays a critical role in thrombosis. What is unclear is the level of enzyme occupancy of FXIIa needed for efficacy, and impact of FXIIa inhibition on cerebral embolism. A selective FXIIa inhibitor, recombinant human albumin-tagged mutant Infestin4 (rHA-Mut-inf), was generated to address these questions. rHA-Mut-inf displayed potency comparable to the original wild-type HA-Infestin4 (rHA-WT-inf) (human FXIIa K_I = 0.07 and 0.12 nM, respectively), with markedly improved selectivity against FXa and plasmin. rHA-Mut-inf binds FXIIa, but not FXII zymogen, and competitively inhibits FXIIa protease activity. Its mode of action is hence akin to typical small molecule inhibitors. Plasma shift and aPTT studies with rHA-Mut-inf demonstrated that calculated enzyme occupancy for FXIIa in achieving a putative aPTT doubling target in human, non-human primate, and rabbit is more than 99.0%. Effects of rHA-Mut-inf in carotid arterial thrombosis and microembolic signal (MES) in middle cerebral artery were assessed simultaneously in rabbits. Dose-dependent inhibition was observed for both arterial thrombosis and MES. The effective dose for 50% inhibition (ED_{50}) of thrombus formation was 0.17 mg/kg rHA-Mut-inf, i.v. for the integrated blood flow and 0.16 mg/kg for thrombus weight; ED_{50} for MES was 0.06 mg/kg. Ex vivo aPTT tracked with efficacy. In summary, our findings demonstrated that very high enzyme occupancy will be required for FXIIa active site inhibitors, highlighting the high potency and exquisite selectivity necessary for achieving efficacy in humans. Our MES studies suggest that targeting FXIIa may offer a promising strategy for stroke prevention associated with thromboembolic events.

Introduction

FXII is the initiator of the intrinsic coagulation cascade and can be activated via contact with charged surfaces to form FXIIa, which then activates FXI and plasma kallikrein. Plasma kallikrein can activate FXII in a reciprocal manner to further amplify contact activation (Renne and Gailani, 2007; Renne et al., 2012; Bjorkqvist et al., 2014). Although human genetics and epidemiological studies to date do not yield a clear relationship between FXII deficiency and risk of thrombosis, FXII deficiency in humans is not associated with bleeding diathesis, despite marked aPTT prolongation (Lammle et al., 1991; Renne and Gailani, 2007). FXII knockout (KO) mice were protected from arterial thrombosis, ischemic stroke, and deep vein thrombosis, while maintaining normal hemostasis (Renne et al., 2005; Kleinschnitz et al., 2006; Muller et al., 2009; von Bruhl et al., 2012), suggesting that FXII is critically involved in pathological thrombus formation but dispensable for hemostasis. Emerging studies also suggest that FXII is a key mediator in host defense and additional immune-inflammatory responses, via its downstream kallikrein/kinin system (KKS) (Schmaier, 2016) and interactions with endothelial and immune cells (Gobel et al., 2016; Long et al., 2016). FXII is thus a promising target for treating not only thrombotic events but also a range of other disorders (Martini et al., 2014; Gobel et al., 2016; Hopp et al., 2016; Nickel et al., 2016; Zamolodchikov et al., 2016) without conferring a bleeding risk.

In recent years, inhibitors for FXII(a) have been generated and described in various preclinical models in vitro or in vivo. These agents include monoclonal antibodies (Larsson et al., 2014; Matafonov et al., 2014), natural peptide or protein inhibitors (Hagedorn et al., 2010; Yau et al., 2012), small molecule inhibitors

(Kleinschnitz et al., 2006; Baeriswyl et al., 2015), RNA aptamer (Woodruff et al., 2013), siRNA (Cai et al., 2015), and antisense oligonucleotide (ASO) (Revenko et al., 2011). While results with these various tool molecules in aggregate strengthen the notion that targeting FXII may provide benefit in a range of disease settings, some of the small molecule or peptide inhibitors utilized in generating in vivo data have insufficient selectivity (Hansson et al., 2014; Korneeva et al., 2014; Xu et al., 2014), hampering the precise understanding on target-based pharmacology. Despite the difficulty in achieving the required target selectivity and potency using a small molecule inhibitor, this modality potentially maintains favorable attributes such as oral bioavailability and shorter pharmacokinetics unavailable in certain other therapeutic classes. As small molecule drugs need to balance between potency, selectivity, and pharmaceutical properties (e.g. permeability and bioavailability), understanding levels of target engagement (e.g. enzyme occupancy, residence time) needed for efficacy is an important component in establishing chemical tractability of the target. The monoclonal antibody modality, while likely carrying a superior selectivity profile, is mechanistically distinct from small molecule inhibitors and is limited in applicable patient settings due to its parenteral route of administration.

It has been observed that FXIIa can be localized to thrombi and can directly interact with fibrin thereby potentially modulating clot structure and thrombus stability (Konings et al., 2011; Kuijpers et al., 2014). While FXII inhibition or loss of function markedly reduces thrombus formation in various models and species, thrombi in $FeCl_3$-injured mesenteric vessels of FXII KO mice appeared unstable and prone to embolization in intravital microscopy studies (Renne et al., 2005), and FXIIa inhibitor treatment has

resulted in increased shedding of emboli in an ultrasound-induced model of atherothrombosis in *Apoe*$^{-/-}$ mice (Kuijpers et al., 2014). As FXII has been proposed to be a target for stroke and other thromboembolic disorders (eg. device-mediated thrombosis in extracorporeal membrane oxygenation and cardiopulmonary bypass) (Dobrovolskaia and McNeil, 2015; Krupka et al., 2016), it is important to further understand the role of FXII in thrombus embolization.

In this report, we set out to examine potency, selectivity, and mode of action of a previously reported FXIIa inhibitor, Inf4mut15 (Campos et al., 2012). We then used this molecule to address two questions: 1) levels of target engagement (calculated enzyme occupancy) needed for FXIIa in generating efficacy; 2) effects of FXIIa inhibition in a novel model of cerebral microembolic signals (MES) induced by $FeCl_3$ injury of the carotid artery in rabbits (Zhou et al., 2016a; Zhou et al., 2016b).

Materials and Methods

Expression and purification of rHA-Mut-inf and rHA-WT-inf

Purified human albumin (HA)-tagged wild-type Infestin-4 (rHA-WT-inf) and mutant Infestin-4 (rHA-Mut-inf) were custom generated by Genscript (Piscataway, NJ, USA) based on the previously reported Infestin-4 (Campos et al., 2004b) and Inf4mut15 (P2 –P4' sequence TRRFVA) (Campos et al., 2012) cDNA sequences, respectively. Recombinant expression methods were as reported earlier (Xu et al., 2014). Briefly, the recombinant pUC57 plasmids containing HA-linker ((Gly-Gly-Ser)^3)-WT- or Mut-inf were transiently transfected into HEK293 cells. Cell culture supernatant was harvested for purification on day 6 post-transfection. The recombinant protein was captured from the cell culture supernatant by Blue Sepharose 6 Fast Flow resin, and eluted in 50 mM

Tris with 3 M NaCl, pH 8.5. The purified protein was buffer-exchanged into Dulbecco's modified PBS (pH 7.0) and analyzed by SDS-PAGE and Western blot with HA antibody (Abcam, Cambridge, MA, USA) for confirmation.

In vitro protease inhibition assays

Human FXIIa, plasma kallikrein, thrombin, aPC, and plasmin were purchased from Enzyme Research Laboratories (South Bend, IN, USA). Human FVIIa, FXIa, and Xa were purchased from Sekisui Diagnostics (Lexington, MA, USA). Human FIXa was purchased from Haematologic Technologies (Essex Junction, VT, USA). Recombinant human tissue plasminogen activator (tPA) was purchased from Hyphen Biomed, S.A.S. (Neuville-sur-Oise, France). Cynomolgus macaque and rabbit FXIIa were prepared by Evotec (US), Inc (Princeton, NJ, USA). The 7-amido-4-thifluoromethylcoumarin (AFC) containing fluorescence substrate, CH_3SO_2-cyclohexyl-Gly-Gly-Arg-AFC (cyclohexyl-G-G-R-AFC) was custom synthesized by CPC Scientific (Sunnyvale, CA, USA), while substrates N-CBZ-Gly-Pro-Arg-AFC (Z-G-P-R-AFC), and n-acetyl-Gly-Pro-Arg-AFC (Acetyl-K-P-R-AFC) were purchased from Sigma-Aldrich (St. Louis, MO, USA).

All enzymatic reactions were carried out in 50 mM HEPES, 150 mM NaCl, 5 mM $CaCl_2$, and 0.1% PEG (8000 NMW), at pH 7.4 and 25°C. The change in fluorescence during reaction progression was monitored using a Tecan m200 plate reader in kinetic mode set at 405 nm excitation and 500 nm emission with 9 and 20 nm bandwidths, respectively. For all enzymes tested except FXIIa the slope of the fluorescence versus time plots was determined by linear regression and plotted versus rHA-Mut-inf concentration to determine IC_{50}, which was subsequently converted to K_I using the Cheng-Prusoff equation. For rHA-Mut-inf and rHA-WT-inf inhibition of human FXIIa,

JPET Fast Forward. Published on December 29, 2016 as DOI: 10.1124/jpet.116.238493
This article has not been copyedited and formatted. The final version may differ from this version.

K_I and binding kinetic parameters (k_{on} and k_{off}) were determined using global progress curve analysis for 1-step slow and tight binding (Zhang and Windsor, 2013). Additional characterization of human, cynomolgus macaque, and rabbit FXIIa activity was performed following a 2 hr pre-incubation of the enzyme with either rHA-WT-inf or rHA-Mut-inf to enable the enzyme-rHA-inf complex to reach equilibrium and analyzed using global progress curve analysis for tight binding.

Plasma Shift Studies

For plasma shifts studies, standard FXIIa enzymatic assays were performed as above described except that either human, cynomolgus, or rabbit FXIIa was preincubated with rHA-Mut-Inf in either the absence or presence of either human, cynomolgus, or rabbit 30% heat-inactivated plasma for 2 hours prior to initiation of the reaction by the addition of substrate. It has been determined that the 30% heat-inactivated plasma retains protein binding activity but is no longer activatable for the endogenous coagulation machinery (not shown). Fluorescence versus time plots were analyzed from global progress curve analysis for 1-step fast and tight binding (Zhang and Windsor, 2013).

To determine the percent unbound concentration of rHA-Mut-inf in 100 % Plasma, % Free, the following equation was used:

$$\%\,Free = \left. 100 \middle/ 1 + \left. \%\,Plasma_{Target} \middle/ \%\,Plasma_{Assay} \right. \times \left(\left. K_{I-app}^{\%\,Plasma_{Assay}} \middle/ K_I \right. - 1 \right) \right.$$

Where $\%\,Plasma_{Target}$ is the target percent plasma (100% in these studies), $\%\,Plasma_{Assay}$ is the percent plasma used in the assay (30% in these studies) and $K_{I-app}^{\%\,Plasma_{Assay}}$ is the plasma shifted K_I.

Surface plasmon resonance

For surface plasmon resonance (SPR) experiments rHA-Mut-inf was immobilized to a standard CM3 sensor chip (GE Healthcare, Piscataway, NJ, USA) using the Amine Coupling Kit and the supplied pH 5.0 sodium acetate buffer to a density of ~2000 RU. Kinetics of binding of FXIIa and FXII zymogen were monitored using the single cycle kinetic method. Running buffer was 10 mM HEPES sodium salt, 150 mM NaCl, 5 mM $CaCl_2$, 0.005 % P-20 at pH 7.4. Solutions of FXIIa and FXII at 0.1, 1, 10, 30, and 100 nM were sequentially injected at a flow rate of 25 μL/min for 240 seconds each. Dissociation was monitored for 3600 seconds following the last injection. Data was analyzed using the 1:1 interaction model and the heterologous ligand model in the BIAcore analysis software. Both fits yielded similar results for the dominant binding event.

Activated partial thromboplastin time (aPTT), prothrombin time (PT), thrombin generation assay (TGA), and thromboelastography (TEG) assay

In vitro and ex vivo activated partial thromboplastin time (aPTT, triggered by aPTT-XL, Pacific Hemostasis, Middletown, VA, USA) and prothrombin time (PT, triggered by TriniCLOT PT Excel, Tcoag, Bray, Ireland) were measured as described before (Xu et al., 2014; Cai et al., 2015).

TGA triggered by 0.83 μM ellagic acid (r2 Diagnostics, South Bend, IN, USA) was performed using standard methods as reported earlier (Xu et al., 2014; Cai et al., 2015). Briefly, rHA-Mut-inf at different concentrations was spiked into 60 μL citrated plasma (human or cynomolgus or rabbit) and incubated at 37°C for 1 hour; 15 μL trigger was then added to the plasma and incubated for an additional 10 minutes at 37°C. 15 μL of FluCa was subsequently injected into the samples to initiate thrombin generation. Thrombinoscope software was used to calculate peak thrombin as well as additional

parameters (lag time, ETP (endogenous thrombin potential), time to peak (ttpeak), and slope (peak divided by the difference between lag and ttpeak)).

TEG analysis was carried out on the thromboelastograph coagulation analyzer model 5000 (Haemonetics, Braintree, MA, USA) as reported earlier (Xu et al., 2013). Briefly, rHA-WT-inf or rHA-Mut-inf at various concentrations was spiked into freshly collected citrated human whole blood and incubated at room temperature for 10 minutes. 340 μL of the blood sample was then transferred into the TEG sample cup preloaded with 20 μL Ca, 3.4 μL ellagic acid, and 1 μL tPA, gently mixed, with the TEG recording initiated right after. The final concentration of ellagic acid in the reaction system was 0.031 μM. Final concentration of tPA in the reaction system was 1.5 nM and this concentration of tPA had been pre-characterized as effectively eliciting a fibrinolysis phase in the donor's blood sample without apparently affecting the coagulation parameters (not shown). R (reaction time), Ly60 (% lysis at 60 minutes post MA) and additional parameters were recorded by the machine and analyzed.

Rabbit microembolic signals (MES) studies

Male New Zealand White rabbits (weighing 2.4–3.0 kg, 10-13 weeks of age, obtained from Charles River Canada), were used for the current studies. All the procedures were conducted in accordance with the Guide for the Care and Use of Laboratory Animals as adopted and promulgated by the U.S. National Institutes of Health, and approved by the Animal Care and Use Committee of Merck & Co., Inc., Kenilworth, NJ USA.

The rabbit model of cerebral MES was induced by $FeCl_3$ injury of the carotid artery as described in detail previously (Zhou et al., 2016a; Zhou et al., 2016b). Briefly,

animals were anesthetized with a cocktail (50 mg/kg ketamine HCl, Pfizer Inc., and 5 mg/kg xylazine, LLOYD Inc., IM) as a non-recovery procedure. The left common carotid artery (CCA) was surgically exposed. A Doppler flow probe (Model 1.5 or 2.0 PRB, Transonic Systems, Ithaca, NY, USA) connected to a flow meter (Model T403, Transonic Systems) was used to measure the artery blood flow with continuous data acquisition by a PowerLab 16/35 and LabChart Pro system (AD Instruments, Colorado Springs, CO, USA). Thrombosis was induced by applying two pieces of filter papers (7.4 mm in diameter, 0.5 mm thick each, above and beneath the vessel; Life Technologies, Grand Island, NY, USA) pre-saturated with 30% FeCl3 (Anhydrous 98%, Cat# 169430050, ACROS Organics/Thermo Fisher Scientific, Waltham, MA, USA) to the adventitial surface of the vessel. A piece of para-film was put underneath the vessel to protect the surrounding tissue from injury. The filter papers were removed after 5 min followed by washout of residue FeCl3 with warm saline. The blood flow was monitored for 60 min from the time of FeCl3 application (as time zero). Integrated carotid blood flow over 60 min was quantitated using area under the curve (AUC), calculated by the trapezoidal rule, and expressed as percent of control blood flow as described previously (Wong et al., 2008; Zhou et al., 2016b). At end of study (i.e., 60 min after $FeCl_3$ injury), the wet thrombus weight was measured using a balance with a detection limit of 0.001 mg (Mettler Toledo Excellence Plus XP Series Analytical Balances, Mettler-Toledo, LLC, Columbus, OH, USA).

The clinical SONARATM TCD System (Nicolet Natus Neurology Inc., Middleton, WI, USA) was used for continuously monitoring the blood flow velocity and MES in the ipsilateral MCA for 60 min upon $FeCl_3$ injury. A pulse wave 2MHz probe

(OD=11.3 mm, 90 mm long, focused at 12 to 25 mm, customized by MTB Medizentechnik Basler AG, Switzerland) was fixed by a flexible-arm magnetic-base holder (McMASTER-CARR, Princeton, NJ, USA) at the posterior end of zygomatic bone of the rabbits, at an angle of ~80 degree against the buccal surface. The MCA was insonated at a depth between 19 to 22 mm as described in details previously (Zhou et al., 2016a). MES (defined as High Intensity Transient Signals, HITS) was saved and further validated based on the criteria defined by the International Consensus Committee as described previously (Ringelstein et al., 1998; Zhou et al., 2016a; Zhou et al., 2016b).

Vehicle (10 mM phosphate buffer, pH 7.0) or various doses of rHA-Mut-inf (0.1-1.0 mg/kg) were administrated at 2 mL/kg, bolus, through the ear vein 20 min prior to the $FeCl_3$ injury. Doses for rHA-Mut-inf were selected based on its comparable potency to rHA-WT-inf in vitro and in our pilot in vivo studies (not shown), and the potency of rHA-WT-inf in our previous studies in rabbits (Xu et al., 2014).

Ex vivo measurement of rHA-Mut-inf plasma concentrations and clotting time assays

Plasma levels of rHA-Mut-inf were measured by a standard liquid chromatography/mass spectrometry (LC/MS) method as reported earlier (Xu et al., 2014) based on the peptide sequence of Mut-inf (Inf4mut15) (Campos et al., 2012).

Ex vivo plasma activated partial thromboplastin time (aPTT) and prothrombin time (PT) were determined by standard methods using aPTT-XL (Pacific Haemostasis, Waltham, MA, USA) and TriniCLOT PT Excel (Tcoag, Bray, Ireland) on a KC4 Delta coagulation analyzer (Tcoag, Bray, Ireland).

Statistical analysis

Data are presented as mean ± standard error (SE), and analyzed using one-way ANOVA followed by Bonferroni post hoc test in GraphPad Prism (Version 7, Graphpad, La Jolla, CA, USA) for comparison among groups with different treatment concentrations or doses. ED50, defined as doses for half-maximal effect, was determined by a non-linear four-parameter dose-response curve fit using GraphPad Prism under the dose ranges described in each figure legend. Results were considered significant when $p < 0.05$.

Results

rHA-Mut-inf is a highly potent and selective inhibitor of FXIIa

Despite its pM potency for FXIIa inhibition, the original rHA-WT-inf carries off-target activity on several other coagulation and fibrinolytic factors including inhibitory activity on FXa and plasmin (Campos et al., 2004b; Xu et al., 2014; Kolyadko et al., 2015). To fully understand the selectivity profile of rHA-Mut-inf we examined its impacts on the enzymatic activities of a comprehensive panel of human and rabbit serine proteases that include coagulation factors, fibrinolytic factors, and trypsin. We chose to determine the apparent inhibition constants (K_I) for all of the enzymes tested (Table 1 and Supplemental Figure 1) in order to accurately assess the occupancy of rHA-Mut-inf for these enzymes in various studies. To facilitate a direct comparison of the activity of these enzymes we used similar fluorescently labeled tripeptide substrates for K_M determinations. For the human enzymes, no less than 4000-fold selectivity was observed for any off-target human enzyme tested and no less than 3200-fold selectivity was observed for rabbit enzyme. Using the same method, K_I for rHA-WT-inf on FXIIa was determined to be 0.12 nM (Supplemental Figure 2). rHA-Mut-inf is thus comparable to

rHA-WT-inf for on-target (FXIIa-inhibitory) activity and is much more selective than rHA-WT-inf against other serine proteases.

Mode of action of rHA-Mut-inf

Fig. 1A shows the inhibitory effects of rHA-Mut-inf on the human FXIIa-mediated cleavage of a fluorescent substrate. As has been previously (Xu et al., 2014) described for rHA-WT-inf, this inhibition is slow to reach equilibrium, and occurs at concentrations of inhibitor less than the concentration of enzyme used for this assay, necessitating taking these factors into account in the analysis of the data to determine the K_I. Also, since under the conditions used in this experiment the time to reach equilibrium was slow relative to the data recording timescale, the binding kinetics of the rHA-Mut-inf−FXIIa interaction has been elucidated directly from this inhibition study. This slowly evolving inhibition is driven by the long half-life of dissociation of the rHA-Mut-inf−FXIIa complex ($t_{1/2}$ = 4.1 h, $k_{off} = 4.8 \times 10^{-5}$ s^{-1}), while the association rate ($k_{on} = 6.6 \times 10^5$ $M^{-1} \bullet s^{-1}$) is within normal ranges for this type of interaction.

Previous studies (Xu et al., 2014; Kolyadko et al., 2015) demonstrated that the inhibition of rHA-WT-inf was not directed against the zymogen FXII, but solely against the activated form (FXIIa). To confirm the activated enzyme specificity and binding kinetics for rHA-Mut-inf we used surface plasmon resonance (SPR) to kinetically monitor the interactions of FXIIa and FXII zymogen with immobilized rHA-Mut-inf (Fig. 1B). Results indicated that rHA-Mut-inf is directed against FXIIa, since no significant binding was observed for zymogen FXII. In addition, kinetic data from SPR (K_D = 250 pM, $k_{on} = 1.0 \times 10^5$ $M^{-1} \bullet s^{-1}$, $k_{off} = 3.0 \times 10^{-5}$ s^{-1}) agree well with the binding kinetics determined directly from the inhibition assays. Furthermore, the mode of FXIIa inhibition

for rHA-Mut-inf was characterized using standard enzymatic methods and shown to be peptide substrate competitive (Fig. 1C). These findings are in accordance with the earlier characterization of rHA-WT-inf mode of inhibition (Xu et al., 2014) and strongly support that the inhibitory effects of these molecules are mediated through their direct interactions with the active site of FXIIa.

Effects of rHA-Mut-inf in aPTT, PT, TGA, and TEG

Functional activity of rHA-Mut-inf was examined in vitro in human, cynomolgus, and rabbit plasma in aPTT and PT assays, as well as in ellagic acid-triggered TGA. rHA-Mut-inf prolonged aPTT in a dose-dependent manner in all 3 species (Fig. 2A), with the potency in rabbit far exceeding that in human and cynomolgus. Concentrations needed for doubling aPTT are 19, 8.5, and 0.26 μM, in human, cynomolgus, and rabbit plasma, respectively. In the PT assay (Fig. 2B), no change in PT was observed at concentrations < 5 μM and a very modest (~10%) PT prolongation was observed in human and cynomolgus plasma at 30 μM. rHA-Mut-inf reduced ellagic acid-triggered thrombin generation in TGA in a dose-dependent manner (Fig. 2C). IC_{50} on peak thrombin is 5.5, 0.69, 0.05 μM in human, cynomolgus, and rabbit plasma, respectively.

Effects of rHA-Mut-inf on blood coagulation and fibrinolysis was also assessed in the whole blood TEG assay (Fig. 3), in a direct comparison with rHA-WT-inf, as described in Methods. A threshold concentration (1.5 nM) of tPA was present in the assay system to generate a fibrinolysis phase without affecting the clotting phase appreciably. Representative TEG traces of the human blood samples treated with 0 (veh), 1, 2, 4 μM rHA-Mut-inf or rHA-WT-inf are shown in Fig. 3A. Both agents exerted a dose-dependent prolongation on R (Fig. 3B, left panel), in a similar manner, with rHA-

Mut-inf being slightly more potent than rHA-WT-inf at the highest concentration tested (4 μM). In contrast, while rHA-WT-inf produced marked and dose-dependent inhibition on tPA-induced fibrinolysis (Ly60), rHA-Mut-inf did not modulate fibrinolysis (Fig. 3B, right panel).

Effects of rHA-Mut-inf in plasma shift studies

An essential component of the calculation of target engagement of a therapeutic molecule is its unbound fraction in the compartment of its target. Since coagulation occurs within the plasma, and since rHA-Mut-inf is a large molecule that is intractable for deriving free fraction in plasma via the conventional equilibrium dialysis method, we assessed the impacts of human, cynomolgus, or rabbit heat-inactivated plasma on the observed inhibition of the respective FXIIa protein by rHA-Mut-inf (Fig. 4 and Table 2) to indirectly determine free fraction in plasma. To minimize the impact of slow-binding by rHA-Mut-inf on the determination of K_I, each species FXIIa was preincubated rHA-Mut-inf for 2 hr, enabling FXIIa•rHA-Mut-inf interactions to reach equilibrium prior to reaction initiation with substrate (Supplemental Figure 3). For each species' plasma, a shift toward lower potency was observed, with the largest shift occurring for human plasma, followed by cynomolgus and the smallest shift observed for rabbit plasma. These shifts were used to estimate the amount of rHA-Mut-inf not bound to plasma proteins and thus available for binding to the target FXIIa (Table 2). From these values the percent of FXIIa bound to rHA-Mut-inf at steady-state was calculated using the concentration of rHA-Mut-inf that prolonged aPTT by 2-fold. 99.2 % target engagement is needed for doubling aPTT in rabbit plasma while 99.9 % target engagement is needed for doubling aPTT in cynomolgus and human plasma.

Effects of rHA-Mut-inf in rabbit MES studies

Dose-dependent inhibition of rHA-Mut-inf on both thrombus formation in the carotid artery and MES incidents in the MCA was observed (Fig. 5). The integrated blood flow (AUC, illustrated as % of blood flow relative to baseline) was increased from 55.0 ± 5.9% in vehicle group (n=8), to 92.3 ± 1.1% for the 1 mg/kg rHA-Mut-inf, i.v. group (n=6, $p<0.01$), with ED_{50} of 0.174 mg/kg rHA-Mut-inf (Fig. 5A and B). Clot weight was reduced from 5.86 ± 0.39 mg (vehicle) to 0.16 ± 0.10 mg (1 mg/kg rHA-Mut-inf, $p<0.001$), with ED_{50} of 0.162 mg/kg rHA-Mut-inf (Fig. 5C).

Fig. 5D illustrates a representative MES recording in the MCA in rabbits treated with 0.1 mg/kg rHA-Mut-inf. The mean MES frequency was reduced from 4.35 ± 1.13 (vehicle) to 0.0 ± 0.0 (1 mg/kg rHA-Mut-inf, $p<0.01$), with ED_{50} of 0.057 mg/kg rHA-Mut-inf (Fig. 5E). The incidence of MES detected in animals was also decreased from 100% (vehicle) to 0% (1 mg/kg rHA-Mut-inf) (Fig. 5F).

Pharmacokinetic and pharmacodynamic analysis of rHA-Mut-inf in the rabbit MES model

Fig. 6A illustrates the dose-related increase in plasma rHA-Mut-inf exposure, with 78.3 ± 3.6, 192.2 ± 10.4, 478.5 ± 47.0 nM observed at 20 min, and 76.3 ± 2.9, 182.1 ± 14.0, 397.8 ± 37.9 nM observed at 80 min, for 0.1, 0.3, 1 mg/kg, i.v bolus dose, respectively. Thus drug exposures during the course of arterial thrombosis and MES monitoring were relatively stable.

Ex vivo aPTT confirmed the pharmacodynamic response for rHA-Mut-inf (Fig. 6B). Significant increase in aPTT was observed for 0.3 and 1 mg/kg rHA-Mut-inf dosing groups. Fold aPTT increase at 0.3 and 1 mg/kg (~1.3-fold and ~2.5-fold, respectively)

with their specific drug exposures are highly consistent with the in vitro spike-in study (Fig. 2A). A very modest numerical increase in PT post-treatment was observed in all treatment groups including vehicle, with the 0.3 and 1 mg/kg groups reaching statistical significance at 80min (Fig. 6C).

Discussion

FXII is an emerging promising target for a number of diseases. rHA-WT-inf has been used extensively for interrogating the role of FXII in thrombosis, hemostasis, and additional pathological settings. However, studies from us (Xu et al., 2014) and others (Kolyadko et al., 2015) demonstrated that rHA-WT-inf carries significant off-target activity on FXa and plasmin that may skew its effect on thrombosis and hemostasis in vivo at high concentrations. We were thus interested in exploring alternative FXIIa inhibitors that may carry an improved selectivity profile. Our in vitro enzyme assays (Table 1) demonstrated that the human albumin (HA) fusion with Inf4mut15, dubbed as rHA-Mut-inf in this report, has comparable on target effect on FXIIa compared to WT-inf, with higher selectivity against FXa and plasmin, consistent with another report of in vitro characterization of the infestin4 mutants without HA fusion (Kolyadko et al., 2015). In the whole blood TEG assay, at 1 and 2 μM, rHA-Mut- and WT-inf prolonged clotting time (R) to the same extent while at 4 μM rHA-Mut-inf was more potent; rHA-Mut-inf did not modulate tPA-induced fibrinolysis whereas rHA-WT-inf dose-dependently suppressed fibrinolysis, likely due to its off-target activity on plasmin. It is possible that at the highest dose (4 μM) tested, strong inhibition of plasmin by rHA-WT-inf has dampened its anticoagulant activity, resulting in a lesser prolongation of R compared to rHA-Mut-inf at 4 μM. While the current tPA-induced fibrinolysis TEG may not mimic

all components in vivo by way of which FXIIa modulates fibrinolysis, the system has been previously benchmarked with a number of thrombin inhibitors with results consistent with expectations (Xu et al., 2013), and the contrast we observed between rHA-Mut- and WT-inf on fibrinolysis is consistent with their in vitro activity on plasmin in a purified system. Overall, these in vitro results demonstrate that rHA-Mut-inf indeed is a much more selective molecule than rHA-WT-inf, consistent with findings from another group using different methods (Kolyadko et al., 2015). As potency of rHA-Mut-inf exceeds that of 3F7 (a monoclonal antibody inhibitor of FXIIa, K_D= 6.2 nM) (Larsson et al., 2014) and FXII618 (a peptide inhibitor of FXIIa, K_I= 22 nM) (Baeriswyl et al., 2015), rHA-Mut-inf is an attractive tool molecule for future research on the role of FXII in vivo in various pathological settings.

With regard to the in vitro aPTT studies, rHA-Mut-inf was much less potent in human and non-human primate plasma as compared to rabbit plasma (Fig. 2A). This is consistent with what was observed with 3F7, and with the hypothesis that FXII-independent activation of FXI may play a more prominent role in primates than in lower species (Gailani et al., 2015). For the in vitro PT studies, appreciable increases in PT were not observed unless at very high concentrations (20-30 μM) and these PT increases could possibly be due to the residual off-target activity of rHA-Mut-inf on FXa, and/or FIIa, and/or FVIIa (Table 1). It is therefore important to monitor the actual exposures of rHA-Mut-inf in order to appropriately interpret results of in vivo studies.

With regard to mode of inhibition, our previous analysis (Xu et al., 2014) as well as X-ray crystallography (Campos et al., 2004a; Campos et al., 2012) and docking studies (Kolyadko et al., 2015) with the active proteases suggest that the infestin family of

peptides act as competitive, reversible inhibitors of the active site of the coagulation factors and additional serine proteases. Our kinetics studies with rHA-Mut-inf using the small tri-peptide substrate (Fig. 1) confirmed this notion. Our SPR-based binding studies (Fig. 1B) further demonstrated that rHA-Mut-inf specifically binds FXIIa but not FXII zymogen. It is therefore unlikely for rHA-Mut-inf to block activation of FXII zymogen to form FXIIa.

As rHA-Mut-inf is a highly selective inhibitor of FXIIa and its mode of inhibition is akin to typical small molecule inhibitors of serine proteases, we were interested in utilizing it in assessing level of target engagement or enzyme occupancy needed for FXIIa for the active site inhibitor mechanism. From drug discovery standpoint, this is a very relevant question, as higher levels of requisite on-target enzyme occupancy will dictate a more stringent selectivity profile and often a higher hurdle on ADME (absorption, distribution, metabolism, excretion) properties of the molecule, especially for an intended oral agent. Using a novel plasma shift assay (Fig. 4), we first determined the % plasma protein binding (likely mediated by HA) for rHA-Mut-inf across species. We then selected a putative target of aPTT doubling in calculating enzyme occupancy. While levels of aPTT prolongation needed for antithrombotic efficacy via targeting FXII in humans are unknown, previous findings with a FXII monoclonal antibody (15H8, targeting heavy chain of FXII) in baboon (Matafonov et al., 2014) suggest that 2X aPTT prolongation is associated with appreciable antithrombotic efficacy in non-human primate and is a reasonable aPTT target, recognizing that aPTT target for translatable efficacy for different modes of inhibition could be different. Calculated enzyme occupancy for FXIIa active site inhibitors for doubling aPTT in human, cynomolgus, and

rabbit plasma was 99.9%, 99.9%, and 99.2%, respectively (Table 2). This is in contrast with the previous findings that 75% ASO-mediated loss of FXII zymogen (Revenko et al., 2011) or 82% siRNA-mediated loss of FXII zymogen (Cai et al., 2015) was sufficient in delivering robust antithrombotic efficacy in various models in rodents, with the caveat that there could be species difference in target-based pharmacology. The very high level of calculated enzyme occupancy needed for FXIIa active site inhibitors is perhaps unsurprising considering that FXIIa is the most upstream factors in the intrinsic cascade and any "leakage" with a tiny amount of FXIIa may be subsequently cascaded and amplified. One precedent of very high level of target engagement for an active site inhibitor of a coagulation factor is apixaban, a FXa inhibitor, requiring >99% calculated enzyme occupancy in order to deliver clinically relevant efficacy (Ankrom et al., 2016). A third potential reason could be that thrombin-mediated activation of FXI will bypass FXII, thus requiring more complete inhibition of FXIIa and immediate shut-down of thrombin generation.

As FXII deficiency confers no bleeding risk, targeting FXII for treatment of ischemic stroke could be a promising strategy. MES has been considered as an independent predictor of stroke or transient ischemic attack (TIA) (Gao et al., 2004; Markus et al., 2005), and MES originated from the carotid artery is considered as one of the primary sources of stroke in patients (Bonati et al., 2010; Yavin et al., 2011). Our findings in the rabbit MES study thus provided preclinical evidence in supporting the therapeutic potential of FXIIa inhibition in the treatment and prevention of ischemic stroke and additional thromboembolic disorders. Our findings also strengthened previous reports on beneficial effects of targeting FXII in cerebral ischemia and reperfusion from

different models and species (Kleinschnitz et al., 2006; Krupka et al., 2016). On the other hand, as more than 2.0X aPTT prolongation was needed to fully restore blood flow in this rabbit MES model (Fig. 5A and 6B), more than 99.0% target engagement will be needed, based on our estimate from in vitro analysis (Table 2). It is to be noted that while our scheme of dosing at 20 minutes prior to vascular injury may ensure adequate and consistent coverage of rHA-Mut-inf during the study based on prior pharmacokinetic study with rHA-WT-inf (Hagedorn et al., 2010), implications of FXIIa inhibition for stroke prophylaxis may need to be further addressed in studies with tool molecules that can allow more flexible dosing paradigms. Another limitation of our study is that neurological deficits and ischemic brain injury could not be assessed under the current experimental setting (i.e., a non-recovery procedure and with FeCl3 injury of the carotid artery for 60 min to end of study).

In summary, rHA-Mut-inf is a highly potent and selective active site inhibitor of FXIIa. Rabbit MES studies with rHA-Mut-inf suggest that FXIIa inhibition may effectively reduce both thrombus formation and thrombus embolization. However, significant challenges in chemical tractability may exist in developing an oral small molecule drug targeting active site of FXIIa. Alternative strategies and alternative mode of inhibition in targeting FXII thus should be considered.

Acknowledgments

We thank Weixun Wang and Xu Wang for analysis of plasma rHA-Mut-inf levels.

Authorship Contributions

Participated in research design: Barbieri, Wang, Seiffert, Gutstein, Chen

Conducted experiments: Barbieri, Wang, Wu, Zhou, Ogawa, O'Neill, Chu, Castriota

Contributed new reagents or analytic tools: Barbieri, Wang, Chen

Performed data analysis: Barbieri, Wang, Wu, Zhou, Ogawa, O'Neill, Chu, Castriota, Chen

Wrote or contributed to the writing of the manuscript: Barbieri, Wang, Seiffert, Gutstein, Chen

References

Ankrom W, Wood HB, Xu J, Geissler W, Bateman T, Chatterjee MS, Feng KI, Metzger JM, Strapps WR, Tadin-Strapps M, Seiffert D and Andre P (2016) Preclinical and translational evaluation of coagulation factor IXa as a novel therapeutic target. *Pharmacol Res Perspect* **4**:e00207.

Baeriswyl V, Calzavarini S, Chen S, Zorzi A, Bologna L, Angelillo-Scherrer A and Heinis C (2015) A Synthetic Factor XIIa Inhibitor Blocks Selectively Intrinsic Coagulation Initiation. *ACS Chem Biol* **10**:1861-1870.

Bjorkqvist J, Nickel KF, Stavrou E and Renne T (2014) In vivo activation and functions of the protease factor XII. *Thrombosis and haemostasis* **112**:868-875.

Bonati LH, Jongen LM, Haller S, Flach HZ, Dobson J, Nederkoorn PJ, Macdonald S, Gaines PA, Waaijer A, Stierli P, Jager HR, Lyrer PA, Kappelle LJ, Wetzel SG, van der Lugt A, Mali WP, Brown MM, van der Worp HB, Engelter ST and group I-Ms (2010) New ischaemic brain lesions on MRI after stenting or endarterectomy for symptomatic carotid stenosis: a substudy of the International Carotid Stenting Study (ICSS). *Lancet Neurol* **9**:353-362.

Cai TQ, Wu W, Shin MK, Xu Y, Jochnowitz N, Zhou Y, Hoos L, Bentley R, Strapps W, Thankappan A, Metzger JM, Ogletree ML, Tadin-Strapps M, Seiffert DA and Chen Z (2015) Factor XII full and partial null in rat confers robust antithrombotic efficacy with no bleeding. *Blood coagulation & fibrinolysis : an international journal in haemostasis and thrombosis* **26**:893-902.

Campos IT, Guimaraes BG, Medrano FJ, Tanaka AS and Barbosa JA (2004a) Crystallization, data collection and phasing of infestin 4, a factor XIIa inhibitor. *Acta crystallographica* **60**:2051-2053.

Campos IT, Souza TA, Torquato RJ, De Marco R, Tanaka-Azevedo AM, Tanaka AS and Barbosa JA (2012) The Kazal-type inhibitors infestins 1 and 4 differ in specificity but are similar in three-dimensional structure. *Acta crystallographica* **68**:695-702.

Campos IT, Tanaka-Azevedo AM and Tanaka AS (2004b) Identification and characterization of a novel factor XIIa inhibitor in the hematophagous insect, Triatoma infestans (Hemiptera: Reduviidae). *FEBS letters* **577**:512-516.

Dobrovolskaia MA and McNeil SE (2015) Safe anticoagulation when heart and lungs are "on vacation". *Ann Transl Med* **3**:S11.

Gailani D, Bane CE and Gruber A (2015) Factor XI and contact activation as targets for antithrombotic therapy. *Journal of thrombosis and haemostasis : JTH* **13**:1383-1395.

Gao S, Wong KS, Hansberg T, Lam WW, Droste DW and Ringelstein EB (2004) Microembolic signal predicts recurrent cerebral ischemic events in acute stroke patients with middle cerebral artery stenosis. *Stroke* **35**:2832-2836.

Gobel K, Pankratz S, Asaridou CM, Herrmann AM, Bittner S, Merker M, Ruck T, Glumm S, Langhauser F, Kraft P, Krug TF, Breuer J, Herold M, Gross CC, Beckmann D, Korb-Pap A, Schuhmann MK, Kuerten S, Mitroulis I, Ruppert C, Nolte MW, Panousis C, Klotz L, Kehrel B, Korn T, Langer HF, Pap T, Nieswandt B, Wiendl H, Chavakis T, Kleinschnitz C and Meuth SG (2016) Blood coagulation factor XII drives adaptive immunity during neuroinflammation via CD87-mediated modulation of dendritic cells. *Nat Commun* **7**:11626.

Hagedorn I, Schmidbauer S, Pleines I, Kleinschnitz C, Kronthaler U, Stoll G, Dickneite G and Nieswandt B (2010) Factor XIIa inhibitor recombinant human albumin Infestin-4 abolishes occlusive arterial thrombus formation without affecting bleeding. *Circulation* **121**:1510-1517.

Hansson KM, Nielsen S, Elg M and Deinum J (2014) The effect of corn trypsin inhibitor and inhibiting antibodies for FXIa and FXIIa on coagulation of plasma and whole blood. *Journal of thrombosis and haemostasis : JTH* **12**:1678-1686.

Hopp S, Albert-Weissenberger C, Mencl S, Bieber M, Schuhmann MK, Stetter C, Nieswandt B, Schmidt PM, Monoranu CM, Alafuzoff I, Marklund N, Nolte MW, Siren AL and Kleinschnitz C (2016) Targeting coagulation factor XII as a novel therapeutic option in brain trauma. *Ann Neurol* **79**:970-982.

Kleinschnitz C, Stoll G, Bendszus M, Schuh K, Pauer HU, Burfeind P, Renne C, Gailani D, Nieswandt B and Renne T (2006) Targeting coagulation factor XII provides protection from pathological thrombosis in cerebral ischemia without interfering with hemostasis. *The Journal of experimental medicine* **203**:513-518.

Kolyadko VN, Lushchekina SV, Vuimo TA, Surov SS, Ovsepyan RA, Korneeva VA, Vorobiev, II, Orlova NA, Minakhin L, Kuznedelov K, Severinov KV, Ataullakhanov FI and Panteleev MA (2015) New Infestin-4 Mutants with Increased Selectivity against Factor XIIa. *PLoS One* **10**:e0144940.

Konings J, Govers-Riemslag JW, Philippou H, Mutch NJ, Borissoff JI, Allan P, Mohan S, Tans G, Ten Cate H and Ariens RA (2011) Factor XIIa regulates the structure of the fibrin clot independently of thrombin generation through direct interaction with fibrin. *Blood* **118**:3942-3951.

Korneeva VA, Trubetskov MM, Korshunova AV, Lushchekina SV, Kolyadko VN, Sergienko OV, Lunin VG, Panteleev MA and Ataullakhanov FI (2014) Interactions outside the proteinase-binding loop contribute significantly to the inhibition of activated coagulation factor XII by its canonical inhibitor from corn. *The Journal of biological chemistry* **289**:14109-14120.

Krupka J, May F, Weimer T, Pragst I, Kleinschnitz C, Stoll G, Panousis C, Dickneite G and Nolte MW (2016) The Coagulation Factor XIIa Inhibitor rHA-Infestin-4 Improves Outcome after Cerebral Ischemia/Reperfusion Injury in Rats. *PLoS One* **11**:e0146783.

Kuijpers MJ, van der Meijden PE, Feijge MA, Mattheij NJ, May F, Govers-Riemslag J, Meijers JC, Heemskerk JW, Renne T and Cosemans JM (2014) Factor XII regulates the pathological process of thrombus formation on ruptured plaques. *Arteriosclerosis, thrombosis, and vascular biology* **34**:1674-1680.

Lammle B, Wuillemin WA, Huber I, Krauskopf M, Zurcher C, Pflugshaupt R and Furlan M (1991) Thromboembolism and bleeding tendency in congenital factor XII deficiency--a study on 74 subjects from 14 Swiss families. *Thrombosis and haemostasis* **65**:117-121.

Larsson M, Rayzman V, Nolte MW, Nickel KF, Bjorkqvist J, Jamsa A, Hardy MP, Fries M, Schmidbauer S, Hedenqvist P, Broome M, Pragst I, Dickneite G, Wilson MJ, Nash AD, Panousis C and Renne T (2014) A factor XIIa inhibitory antibody provides thromboprotection in extracorporeal circulation without increasing bleeding risk. *Science translational medicine* **6**:222ra217.

Long AT, Kenne E, Jung R, Fuchs TA and Renne T (2016) Contact system revisited: an interface between inflammation, coagulation, and innate immunity. *Journal of thrombosis and haemostasis : JTH* **14**:427-437.

Markus HS, Droste DW, Kaps M, Larrue V, Lees KR, Siebler M and Ringelstein EB (2005) Dual antiplatelet therapy with clopidogrel and aspirin in symptomatic carotid stenosis evaluated using doppler embolic signal detection: the Clopidogrel and Aspirin for Reduction of Emboli in Symptomatic Carotid Stenosis (CARESS) trial. *Circulation* **111**:2233-2240.

Martini S, Nair V, Keller BJ, Eichinger F, Hawkins JJ, Randolph A, Boger CA, Gadegbeku CA, Fox CS, Cohen CD, Kretzler M, European Renal c DNAB, Cohort CP and Consortium CK (2014) Integrative biology identifies shared transcriptional networks in CKD. *Journal of the American Society of Nephrology : JASN* **25**:2559-2572.

Matafonov A, Leung PY, Gailani AE, Grach SL, Puy C, Cheng Q, Sun MF, McCarty OJ, Tucker EI, Kataoka H, Renne T, Morrissey JH, Gruber A and Gailani D (2014) Factor XII inhibition reduces thrombus formation in a primate thrombosis model. *Blood* **123**:1739-1746.

Muller F, Mutch NJ, Schenk WA, Smith SA, Esterl L, Spronk HM, Schmidbauer S, Gahl WA, Morrissey JH and Renne T (2009) Platelet polyphosphates are proinflammatory and procoagulant mediators in vivo. *Cell* **139**:1143-1156.

Nickel KF, Labberton L, Long AT, Langer F, Fuchs TA, Stavrou EX, Butler LM and Renne T (2016) The polyphosphate/factor XII pathway in cancer-associated thrombosis: novel perspectives for safe anticoagulation in patients with malignancies. *Thrombosis research* **141 Suppl 2**:S4-7.

Renne T and Gailani D (2007) Role of Factor XII in hemostasis and thrombosis: clinical implications. *Expert review of cardiovascular therapy* **5**:733-741.

Renne T, Pozgajova M, Gruner S, Schuh K, Pauer HU, Burfeind P, Gailani D and Nieswandt B (2005) Defective thrombus formation in mice lacking coagulation factor XII. *The Journal of experimental medicine* **202**:271-281.

Renne T, Schmaier AH, Nickel KF, Blomback M and Maas C (2012) In vivo roles of factor XII. *Blood* **120**:4296-4303.

Revenko AS, Gao D, Crosby JR, Bhattacharjee G, Zhao C, May C, Gailani D, Monia BP and MacLeod AR (2011) Selective depletion of plasma prekallikrein or coagulation factor XII inhibits thrombosis in mice without increased risk of bleeding. *Blood* **118**:5302-5311.

Ringelstein EB, Droste DW, Babikian VL, Evans DH, Grosset DG, Kaps M, Markus HS, Russell D and Siebler M (1998) Consensus on microembolus detection by TCD. International Consensus Group on Microembolus Detection. *Stroke* **29**:725-729.

Schmaier AH (2016) The contact activation and kallikrein/kinin systems: pathophysiologic and physiologic activities. *Journal of thrombosis and haemostasis : JTH* **14**:28-39.

von Bruhl ML, Stark K, Steinhart A, Chandraratne S, Konrad I, Lorenz M, Khandoga A, Tirniceriu A, Coletti R, Kollnberger M, Byrne RA, Laitinen I, Walch A, Brill A, Pfeiler S, Manukyan D, Braun S, Lange P, Riegger J, Ware J, Eckart A, Haidari S, Rudelius M, Schulz C, Echtler K, Brinkmann V, Schwaiger M, Preissner KT, Wagner DD, Mackman N, Engelmann B and Massberg S (2012) Monocytes,

neutrophils, and platelets cooperate to initiate and propagate venous thrombosis in mice in vivo. *The Journal of experimental medicine* **209**:819-835.

Wong PC, Watson CA and Crain EJ (2008) Arterial antithrombotic and bleeding time effects of apixaban, a direct factor Xa inhibitor, in combination with antiplatelet therapy in rabbits. *Journal of thrombosis and haemostasis : JTH* **6**:1736-1741.

Woodruff RS, Xu Y, Layzer J, Wu W, Ogletree ML and Sullenger BA (2013) Inhibiting the intrinsic pathway of coagulation with a factor XII-targeting RNA aptamer. *Journal of thrombosis and haemostasis : JTH* **11**:1364-1373.

Xu Y, Cai TQ, Castriota G, Zhou Y, Hoos L, Jochnowitz N, Loewrigkeit C, Cook JA, Wickham A, Metzger JM, Ogletree ML, Seiffert DA and Chen Z (2014) Factor XIIa inhibition by Infestin-4: in vitro mode of action and in vivo antithrombotic benefit. *Thrombosis and haemostasis* **111**:694-704.

Xu Y, Wu W, Wang L, Chintala M, Plump AS, Ogletree ML and Chen Z (2013) Differential profiles of thrombin inhibitors (heparin, hirudin, bivalirudin, and dabigatran) in the thrombin generation assay and thromboelastography in vitro. *Blood coagulation & fibrinolysis : an international journal in haemostasis and thrombosis* **24**:332-338.

Yau JW, Stafford AR, Liao P, Fredenburgh JC, Roberts R, Brash JL and Weitz JI (2012) Corn trypsin inhibitor coating attenuates the prothrombotic properties of catheters in vitro and in vivo. *Acta biomaterialia* **8**:4092-4100.

Yavin D, Roberts DJ, Tso M, Sutherland GR, Eliasziw M and Wong JH (2011) Carotid endarterectomy versus stenting: a meta-analysis of randomized trials. *Can J Neurol Sci* **38**:230-235.

Zamolodchikov D, Renne T and Strickland S (2016) The Alzheimer's disease peptide beta-amyloid promotes thrombin generation through activation of coagulation factor XII. *Journal of thrombosis and haemostasis : JTH* **14**:995-1007.

Zhang R and Windsor WT (2013) In vitro kinetic profiling of hepatitis C virus NS3 protease inhibitors by progress curve analysis. *Methods in molecular biology* **1030**:59-79.

Zhou X, Kurowski S, Wu W, Desai K, Chu L, Gutstein DE, Seiffert D and Wang X (2016a) A Rabbit Model of Cerebral Microembolic Signals for Translational Research: Preclinical Validation for Aspirin and Clopidogrel. *Journal of thrombosis and haemostasis : JTH*.

Zhou X, Wu W, Chu L, Gutstein DE, Seiffert D and Wang X (2016b) Apixaban Inhibits Cerebral Microembolic Signals Derived from Carotid Arterial Thrombosis in Rabbits. *The Journal of pharmacology and experimental therapeutics*.

Figure Legends

Fig. 1. ***rHA-Mut-inf inhibits FXIIa specifically and reversibly with pM potency.*** A. Time course of inhibition of FXIIa proteolysis of fluorescent substrate by rHA-Mut-inf. Concentrations in nM of rHA-Mut-inf are indicated. Solid lines represent the nonlinear least squares analysis of the data as described in Materials and Methods. B. Direct measurement of the interaction between rHA-Mut-inf and FXIIa (filled circles), or between rHA-Mut-inf and FXII zymogen (open circles), via SPR. C. Assessment of the mechanism of inhibition of FXIIa by rHA-Mut-inf. Solid lines represent the global analysis of the data using a model for competitive inhibition. Inset is the double reciprocal plot of the same data, clearly indicating competitive inhibition. Concentrations in nM of rHA-Mut-inf are indicated. Individual plots shown are representative of replicate experiments, n = 4, n = 2, and n = 3, panels A, B, and C, respectively.

Fig. 2. ***rHA-Mut-inf markedly prolonged aPTT and reduced intrinsic-triggered thrombin generation in plasma with substantially more pronounced effects in rabbit than in higher species.*** rHA-Mut-inf at different concentrations were spiked into human, cynomolgus, and rabbit plasma (black, red, green, respectively) for aPTT (A), PT (B), and ellagic acid-triggered TGA (C) analyses. aPTT, PT, and TGA were conducted using standard methods as described in Materials and Methods. Individual plots shown are representative of replicate experiments, n = 2, n = 2, and n = 2, panels A, B, and C, respectively.

Fig. 3. ***Unlike rHA-WT-inf, rHA-Mut-inf does not modulate fibrinolysis in the fibrinolysis TEG.*** Both compounds were spiked at varying concentrations into freshly collected citrated human whole blood and subjected to ellagic acid-triggered TEG in the

presence of tPA, as described in Methods. n = 6 individual donors. A. TEG traces post-treatment with rHA-Mut-inf (left) and rHA-WT-inf (right) from one representative donor. B. Summary result of effects of the 2 compounds on clotting time (R, left graph), and on fibrinolysis (%Ly60, right graph). **p<0.01, and ***p<0.001 vs. vehicle (0 μM).

Fig. 4. ***rHA-Mut-inf interacts with plasma causing an apparent decrease in inhibition of FXIIa activity.*** Inhibition of human, cynomolgus, and rabbit FXIIa activity (A, B, and C, respectively) by rHA-Mut-inf, in the absence (black) or presence (red) of 30% heat-inactivated species-specific plasma. Individual plots shown are representative of replicate experiments, n = 4, n = 2, and n = 4, panels A, B, and C, respectively.

Fig. 5. ***Dose-dependent effect of rHA-Mut-inf on $FeCl_3$-induced arterial thrombosis and cerebral MES.*** rHA-Mut-inf dose-dependently inhibited 30% $FeCl_3$-induced carotid arterial thrombosis (vehicle, n=8; 0.1, n=8; 0.3, n=9; and 1.0 mg/kg, n=6, i.v.) as illustrated using carotid blood flow within 60 min upon $FeCl_3$ injury (A), AUC of the integrated blood flow (B), and reduction in clot weight (C). MES was monitored simultaneously in the ipsilateral MCA to the $FeCl_3$ injury. Representative image for MES detection by TCD in vehicle treated animal is illustrated with a snapshot of TCD recording in a period of 4 seconds (D). The MES was indicated in an arrow determined by the Sonora software and confirmed manually. Mean frequency (E) and incidence of MES (F) in MCA was also dose-dependently reduced. *p<0.05, **p<0.01, and ***p<0.001 vs. vehicle.

Fig. 6. ***Pharmacokinetic and pharmacodynamics responses for rHA-Mut-inf treatment on $FeCl_3$-induced arterial thrombosis and cerebral MES.*** Plasma samples were prepared in animals of each experimental group in Fig. 5 prior to, or 20 min (time of

$FeCl_3$ injury) and 80 min after rHA-Mut-inf i.v. bolus dosing. n = 8, 8, 9, 6, for the vehicle, 0.1, 0.3, and 1.0 mg/kg treatment group, respectively. Plasma drug exposures are illustrated in A. Ex vivo aPTT and PT are depicted in B and C, respectively. Statistical analyses for aPTT and PT were conducted for each dosing group in comparison with its own baseline. **p<0.01, ***p<0.001 vs. respective baselines.

JPET Fast Forward. Published on December 29, 2016 as DOI: 10.1124/jpet.116.238493
This article has not been copyedited and formatted. The final version may differ from this version.

***Table 1*. rHA-Mut-inf is highly selective for FXIIa over other enzymes involved in coagulation and fibrinolysis**

Enzyme	Organism	K_I (nM)	[b]Fold Selectivity	Substrate	[Substrate] (mM)	K_M (mM)
FXIIa	Human	0.07[a]	1	Acetyl-K-P-R-AFC	0.1	0.78
	Rabbit	0.22[a]	1		0.1	0.72
FXa	Human	30000	430000	Acetyl-K-P-R-AFC	0.1	2.6
	Rabbit	700	3200		0.08	2.3
FIIa	Human	>5000	>77000	Acetyl-K-P-R-AFC	0.05	0.05
	Rabbit	>15000	>146000		0.08	0.08
FXIa	Human	9000	130000	Z-G-P-R-AFC	0.1	0.1
	Rabbit	>26000	>120000		0.08	0.60
tPA	Human	>8100	>120000	Cyclohexyl G-G-R-AFC	0.25	1.1
	Rabbit	>26000	>120000		0.25	1.4
plasmin	Human	1650	24000	Acetyl-K-P-R-AFC	0.1	3.5
	Rabbit	3300	15000		0.08	0.94
kallikrein	Human	>8500	>120000	Acetyl-K-P-R-AFC	0.1	0.58
	Rabbit	3530	16000		0.08	0.88
FVIIa	Human	98200	1000000	Acetyl-K-P-R-AFC	0.1	5.4
	Rabbit	>29000	>130000		0.08	2.6
FIXa	Human	>9500	>140000	Cyclohexyl G-G-R-AFC	0.25	>5mM
aPC	Human	>9100	>130000	Cyclohexyl G-G-R-AFC	0.25	2.5
uPA	Human	>7600	>110000	Cyclohexyl G-G-R-AFC	0.25	0.80
	Rabbit	>26000	>120000	Acetyl-K-P-R-AFC	0.08	0.53
trypsin	Human	285	4000	Acetyl-K-P-R-AFC	0.025	0.025

[a] As described in the legend to Fig 2. rHA-Mut-inf inhibition of FXIIa is time dependent and inhibition constant (K_i) was determined using global analysis of reaction progress curves to determine K_i and binding-kinetics parameters. All other enzymatic assays displayed zero-order kinetics in the presence of rHA-Mut-inf and were analyzed using standard methods.

[b] Fold selectivity is the difference in K_I of rHA-Mut-inf for the indicated enzyme versus the K_I of rHA-Mut-inf for FXIIa from either human or rabbit FXIIa, respectively.

JPET Fast Forward. Published on December 29, 2016 as DOI: 10.1124/jpet.116.238493
This article has not been copyedited and formatted. The final version may differ from this version.

Table 2. **Enzyme occupancy for FXIIa in 3 species for a putative target of aPTT doubling**

Species	K_I (nM)	[a] $K_{I\text{-app 30\% plasma}}$ (nM)	[b] % Free in 100% Plasma	[c] [rHA-Mut-inf] at 2X aPTT (nM)	[d] % $XIIa_{Bound}$ at 2X aPTT
Human	0.08	4.19	0.55 %	19000	99.93 %
Cyno	0.20	2.05	3.21 %	8500	99.93 %
Rabbit	0.22	0.82	9.97 %	260	99.15 %

[a] $K_{I\text{-app 30\% plasma}}$ indicates the value of K_I observed in the presence of 30 % heat-inactivated plasma.

[b] % Free in 100% Plasma is the estimated using the equation described in the materials and methods

[c] [Mut-inf] at 2X aPTT is the concentration of rHA-Mut-inf associated with a 2-fold increase in aPTT time.

[d] % $XIIa_{Bound}$ at 2X aPTT is the percent of XIIa in complex with rHA-Mut-inf at concentration yielding 2X aPTT.

Figure 1

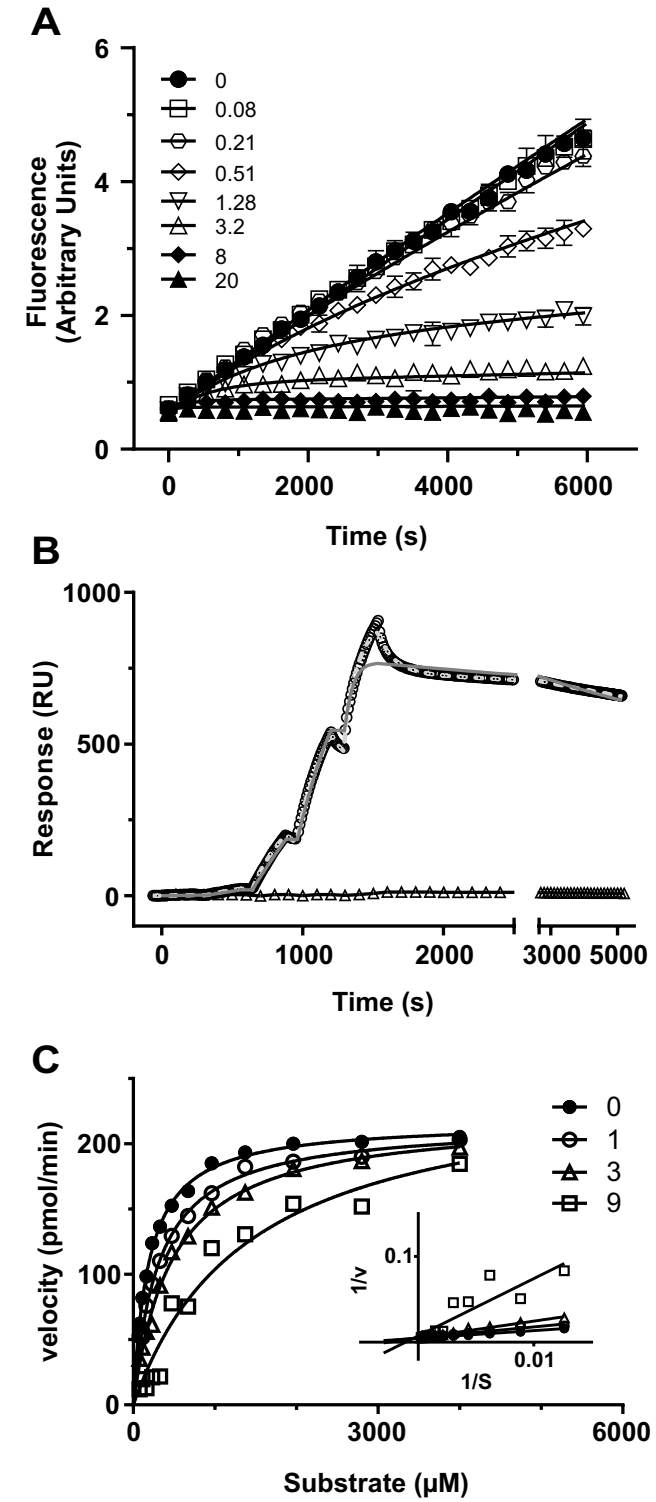
A
Fluorescence (Arbitrary Units)
0
2
4
6
0
0.08
0.21
0.51
1.28
3.2
8
20
0
2000
4000
6000
Time (s)
B
Response (RU)
0
500
1000
0
1000
2000
3000
5000
Time (s)
C
velocity (pmol/min)
0
100
200
0
3000
6000
Substrate (μM)
0
1
3
9
1/v
0.1
1/S
0.01

Figure 2

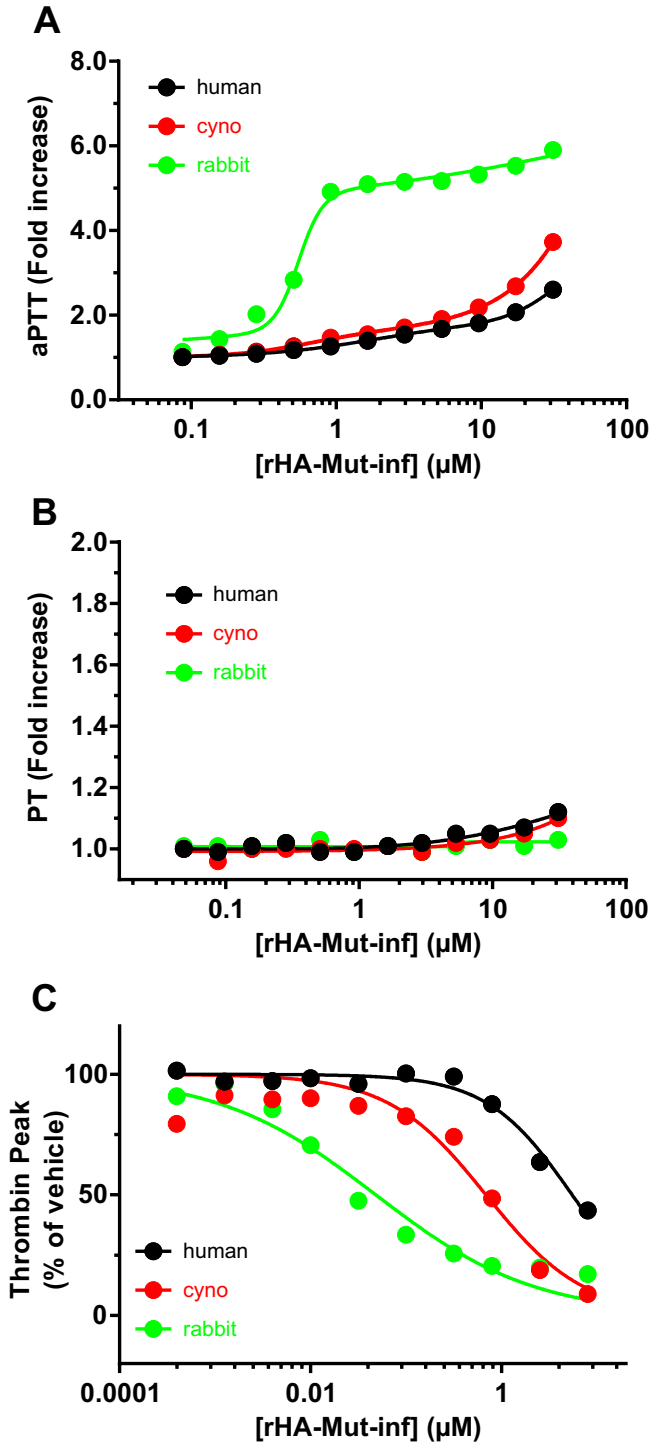
A
aPTT (Fold increase)
8.0
6.0
4.0
2.0
0.0
human
cyno
rabbit
0.1
1
10
100
[rHA-Mut-inf] (μM)
B
PT (Fold increase)
2.0
1.8
1.6
1.4
1.2
1.0
human
cyno
rabbit
0.1
1
10
100
[rHA-Mut-inf] (μM)
C
Thrombin Peak
(% of vehicle)
100
50
0
human
cyno
rabbit
0.0001
0.01
1
[rHA-Mut-inf] (μM)

Figure 3

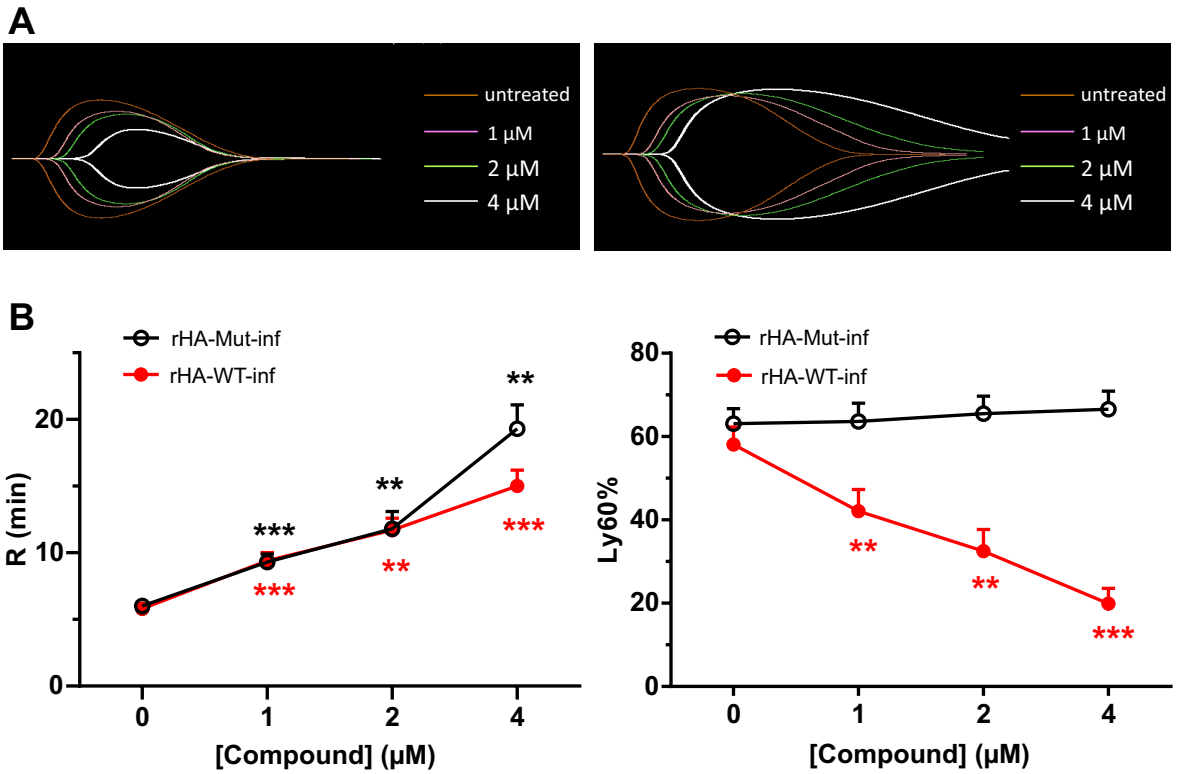
A
untreated
1 µM
2 µM
4 µM
untreated
1 µM
2 µM
4 µM
B
rHA-Mut-inf
rHA-WT-inf
R (min)
20
10
0
0
1
2
4
[Compound] (µM)
**
**
***
***
**
***
rHA-Mut-inf
rHA-WT-inf
Ly60%
80
60
40
20
0
0
1
2
4
[Compound] (µM)
**
**
***

Figure 4

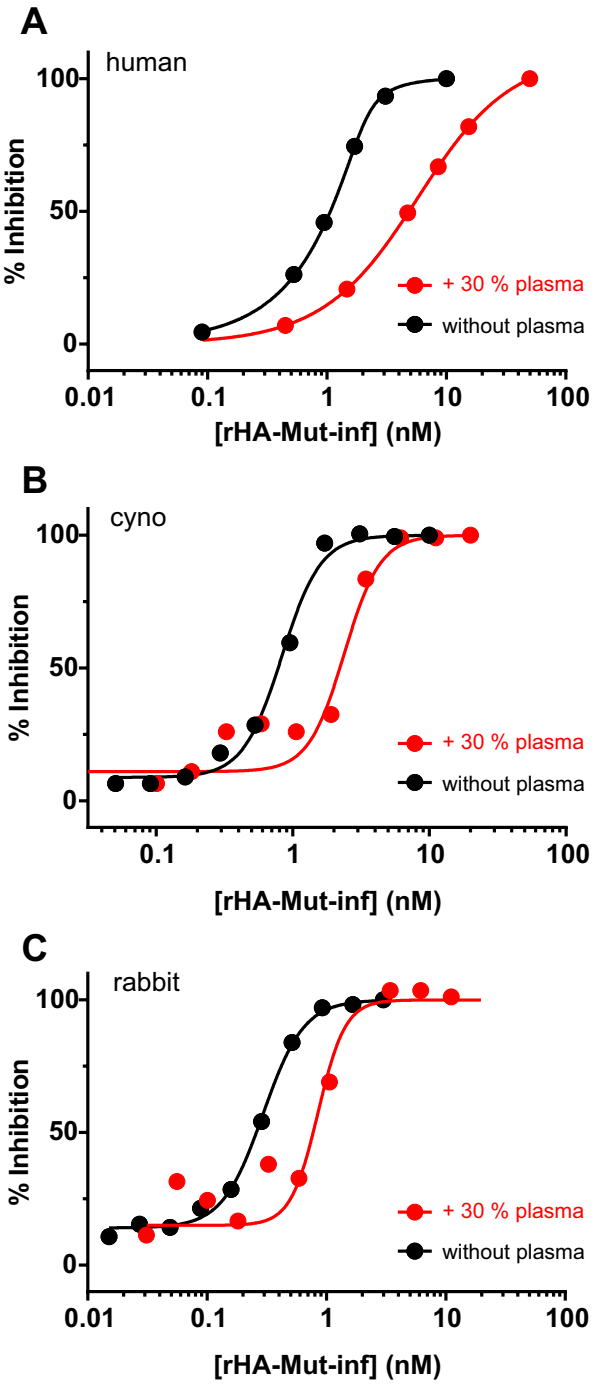
A
human
100
50
0
% Inhibition
+ 30 % plasma
without plasma
0.01
0.1
1
10
100
[rHA-Mut-inf] (nM)
B
cyno
100
50
0
% Inhibition
+ 30 % plasma
without plasma
0.1
1
10
100
[rHA-Mut-inf] (nM)
C
rabbit
100
50
0
% Inhibition
+ 30 % plasma
without plasma
0.01
0.1
1
10
100
[rHA-Mut-inf] (nM)

Figure 5

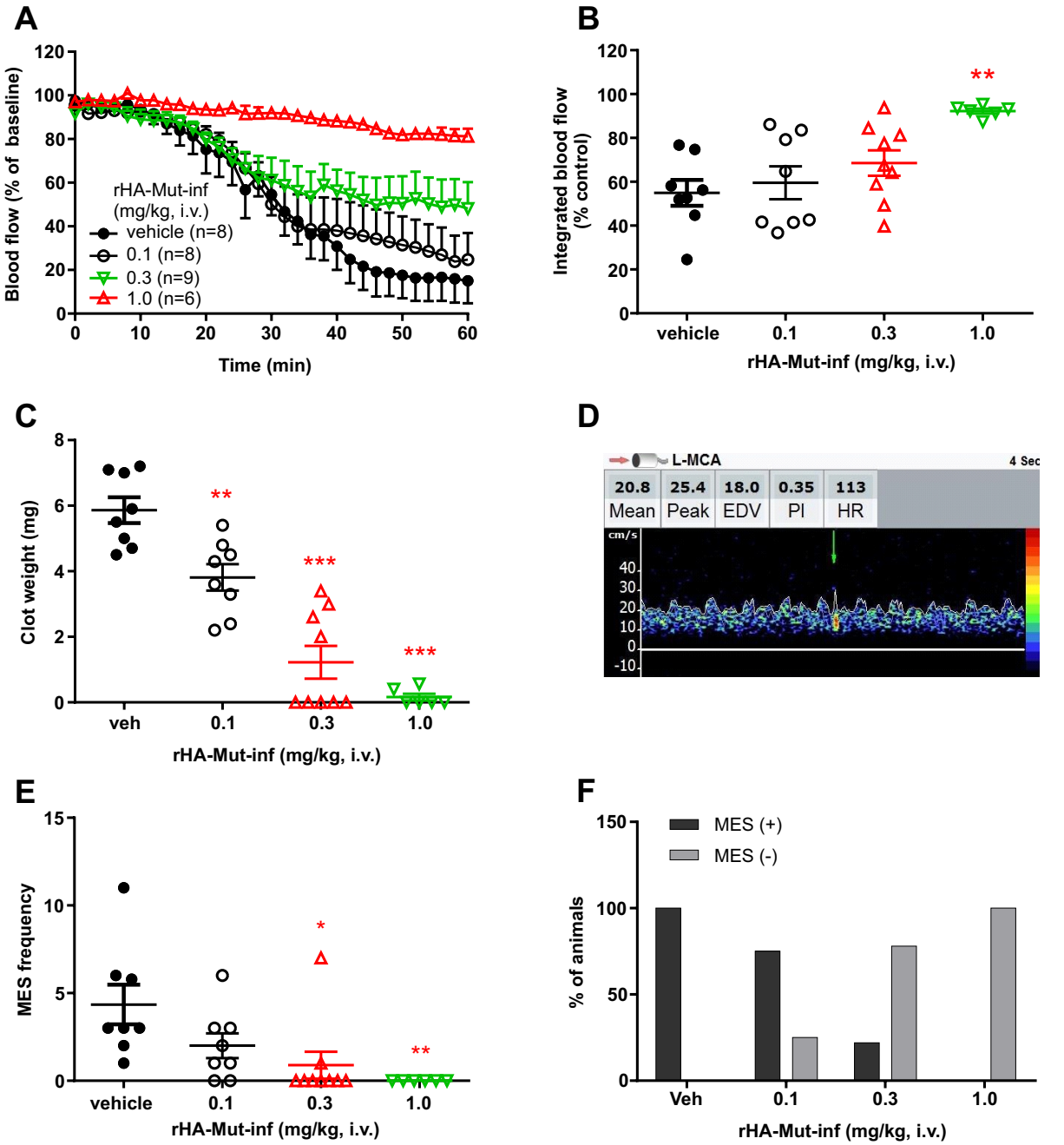
A
Blood flow (% of baseline)
Time (min)
rHA-Mut-inf (mg/kg, i.v.)
vehicle (n=8)
0.1 (n=8)
0.3 (n=9)
1.0 (n=6)
B
Integrated blood flow (% control)
rHA-Mut-inf (mg/kg, i.v.)
vehicle
0.1
0.3
1.0
C
Clot weight (mg)
rHA-Mut-inf (mg/kg, i.v.)
veh
D
L-MCA
4 Sec
Mean
Peak
EDV
PI
HR
cm/s
E
MES frequency
rHA-Mut-inf (mg/kg, i.v.)
F
MES (+)
MES (-)
% of animals
Veh
rHA-Mut-inf (mg/kg, i.v.)

Figure 6

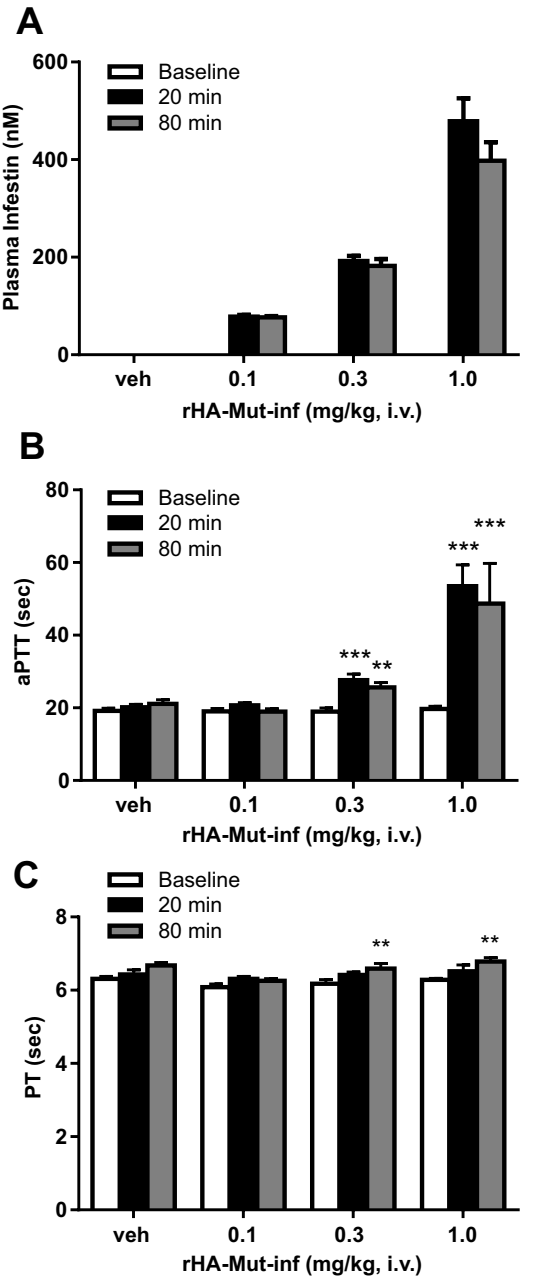
A
Plasma Infestin (nM)
600
400
200
0
Baseline
20 min
80 min
veh
0.1
0.3
1.0
rHA-Mut-inf (mg/kg, i.v.)
B
aPTT (sec)
80
60
40
20
0
***
**
***
***
C
PT (sec)
8
6
4
2
0
**
**